ELSEVIER

Journal of Marine Systems 35 (2002) 99–110

JOURNAL OF MARINE SYSTEMS

www.elsevier.com/locate/jmarsys

# On advection and diffusion of plankton in coarse resolution ocean models

Göran Broström*

*Department of Earth, Atmospheric and Planetary Sciences, Massachusetts Institute of Technology, Cambridge, MA 02139, USA*

Received 16 October 2000; accepted 30 January 2002

**Abstract**

There is a widespread use of general circulation models (GCMs) to study the importance of various physical and biological processes for the primary production, and to understand the structure of the oceanic food web. However, it is shown that low-resolution GCMs may produce too high advection speeds for a plankton bloom that invade an area with potentially high plankton growth rates. Under the prescribed situation, the advection and diffusion act to initiate an exponential growth of plankton in a large grid cell implying that the plankton signal is quickly carried over the entire grid cell. When a certain concentration is reached, it may seed the surrounding grid cells with phytoplankton, and the procedure is repeated. Accordingly, the phytoplankton bloom can travel faster in the low-resolution model than the ocean currents that carry them. Some numerical experiments show that the resolution of the model needs to be at least on the order of $\Delta x \sim U/\gamma_P$ or $\sqrt{D/\gamma_P}$—whichever is largest—to describe the plankton dynamics in an adequate way. Here, $U$ is the typical horizontal advection velocity, $D$ is the horizontal diffusivity for plankton, and $\gamma_P$ represents the growth rate of phytoplankton. With $U=0.1$ m/s and $\gamma_P=1$ day$^{-1}$, it follows that the resolution needs to be at least 8 km to describe the phytoplankton dynamics in a reasonably correct way. Most GCM experiments use coarser resolution; accordingly, the results regarding the advection of plankton in these models should thus be viewed with some caution. 

*Keywords:* Plankton dynamics; Advection; Diffusion; GCM models; Coarse resolution

## 1. Introduction

Ecosystem modeling is a powerful way to interpolate and extrapolate measurements on biological variables to a more general context (Doney et al., 1996; Evans and Parslow, 1985; Fasham et al., 1990, 1993; McGillicuddy et al., 1995). An important part of the modeling approach is to describe the physical properties of the system in an adequate way. Any caveats in the description of the physics will cast doubts on the robustness of the model results and, consequently, on the interpretation of the model dynamics. Thus, if advection and diffusion are described incorrectly, the use of model results to interpret measurements may be erroneous.

The development in ocean models provides us with a powerful tool to describe the general circulation of the oceans in a consistent way (Marshall et al., 1997a,b; McGillicuddy and Robinson, 1998; Oberhuber, 1993; Stammer et al., 1997). Accordingly, it is useful to couple a biological model with a realistic

* Department of Oceanography, Earth Science Centre, Göteborg University, Box 460, S-405 30 Gothenburg, Sweden. Fax: +46-31-774-2888.

*E-mail address:* gobr@oce.gu.se (G. Broström).

0924-7963/02/$ - see front matter 
PII: S0924-7963(02)00078-7

general circulation model (GCM) to gain insights in the importance of various physical properties on the ecosystem dynamics (Fasham et al., 1993; McGillicuddy et al., 1998, 1995; Oschlies and Garcon, 1998).

However, although most GCMs provide a reasonable description of the physical properties of the ocean, it is shown that coarse resolution models may not provide a realistic framework for the transport of plankton under some circumstances. Let us consider an area with high potential growth rate for a specific phytoplankton, but where the growth is limited by the absence of plankton. Plankton is carried by the ocean currents and should invade the plankton-free area with approximately the speed of the ocean currents. However, if there is a sharp front in a low-resolution model, the advection and diffusion act to initiate a seed population in the neighboring boxes, which phytoplankton start to grow at an exponential rate. Once the box reach a large phytoplankton population, it will seed the neighboring boxes with phytoplankton, and the signal propagates to the next box. The result is that the front of the phytoplankton bloom may travel significantly faster than the ocean currents. Further, the speed of the plankton front depends on the resolution of the model rather than any physical properties of the system.

Some results from a simple phytoplankton model that includes advection and diffusion are described in Section 2. A few experiments with the MIT GCM model are illustrated in Section 3; these experiments provide a platform for the discussion given in Section 4.

## 2. The advection, diffusion and growth of phytoplankton

### 2.1. Basic equation

Let us consider the following model for the phytoplankton concentration, $P$,

$$\frac{\partial P}{\partial t} + U\frac{\partial P}{\partial x} = D\frac{\partial^2 P}{\partial x^2} + \gamma_P P - \mu_P P^2, \tag{1}$$

where $U$ is the speed of the ocean current, and $D$ is the horizontal diffusivity in the ocean. The rate of change of the phytoplankton is thus given by the following factors: the advective transport of plankton; diffusion of plankton; the growth of plankton, characterized by the growth parameter, $\gamma_P$; and losses by grazing/metabolism as specified by the loss parameter, $\mu_P$. The quadratic loss term mimics the situation where the grazing rate and the zooplankton population both depend linearly on the phytoplankton concentration. It should be noted that some numerical schemes might occasionally produce negative phytoplankton concentrations; in this case, the growth and metabolism of plankton are set to zero.

In principle, nutrients should be included in the plankton model. However, in the initial part of the spring bloom, there are generally high nutrient concentrations, and the plankton growth is not limited by nutrients. In fact, at ocean weather stations M (66°N, 2°E), C (52°N, 35°W), I (59°N, 19°W), and P (50°N, 145°W), the nutrient concentrations decrease rather slowly after the initial part of the spring bloom reaching low values say 2 months after the start of the bloom (Broström, 2000; Broström and Drange, 2000; Fasham, 1995; Sambrotto et al., 1993).

To simplify the discussions, the following nondimensional variables are introduced:

$$P = \frac{\gamma_P}{\mu_P}P',\ t = \frac{1}{\gamma_P}t',\ x = \frac{U}{\gamma_P}x'. \tag{2a – c}$$

These variables cast Eq. (1) into the following simple form

$$\frac{\partial P}{\partial t} + \frac{\partial P}{\partial x} = \alpha\frac{\partial^2 P}{\partial x^2} + P(1-P), \tag{3}$$

where the primes have been dropped and

$$\alpha = \frac{D\gamma_P}{U^2}.$$

Here, $\alpha$ is a nondimensional parameter that measures the strength of the diffusion and the phytoplankton growth relative to the advection. The diffusivity in the ocean is generally small as compared to the strength of the advection, and $\alpha = 0.1$ will be used in this study. Notably, Eq. (3) has two quasi-steady solutions: $P = 0$ and $P \approx 1$. It is notable that the $P = 0$ solution is unstable to infinitesimal disturbances. However, there must be an initial disturbance, and it may take some time to reach the $P \approx 1$ solution if the initial disturbance is small.

### 2.2. Similarity solution

Eq. (3) is known as the Fisher equation and has been studied extensively in population dynamics (Murray, 1989). The Fisher equation has a traveling wave solution of the form

$$P(t,x) = \Pi(\xi), \tag{4a}$$

where

$$\xi = x - ct. \tag{4b}$$

The phase speed of the traveling wave solution, $c$, is given by $c = 1 + 2\sqrt{\alpha}$. In most experiments, $\alpha = 0.1$ will be used which implies that $c \approx 1.63$. There is no guarantee that the traveling wave solution exists for all possible initial conditions. However, the numerical experiments presented in this study show that the traveling wave solution exists for the present initial conditions. The form of the solution is described by

$$\alpha\Pi''(\xi) + c\Pi'(\xi) = \Pi(\xi)(1 - \Pi(\xi)). \tag{5}$$

It is not possible to find an exact analytical solution to Eq. (5). However, it is possible to find an approximate solution by (i) setting the advection velocity to zero, (ii) by neglecting the second order derivative in Eq. (5). The approximate solution, defined such that $\Pi(0) = 0.5$, may be written as (Murray, 1989)

$$\Pi(\xi) = (1 + e^{\xi/2\sqrt{\alpha}})^{-1}. \tag{6}$$

The forms of the front for a few values of $\alpha$ are shown in Fig. 1. The analytical approximation described in Eq. (6) fits a high-resolution numerical solution very well. With small values on $\alpha$ the plankton form is steep and the plankton bloom travels slow, and with large values on $\alpha$ the front is flatter and the plankton front travels faster. The maximum gradient according to Eq. (6) is $(8\sqrt{\alpha})^{-1}$, the numerical resolution should thus be of order $\sqrt{\alpha}$ to resolve the plankton front in a correct way (it appears that a resolution of say $3\sqrt{\alpha}$ may be sufficient to describe the front reasonably well, this is also confirmed by some numerical experiments). This resolution is higher than used in most GCMs, and it is relevant to study the numerical properties of the solution when the plankton front is not resolved in the model. Further, Eq. (6) do not provide any information on the resolution required to describe the advection of plankton in a proper way.

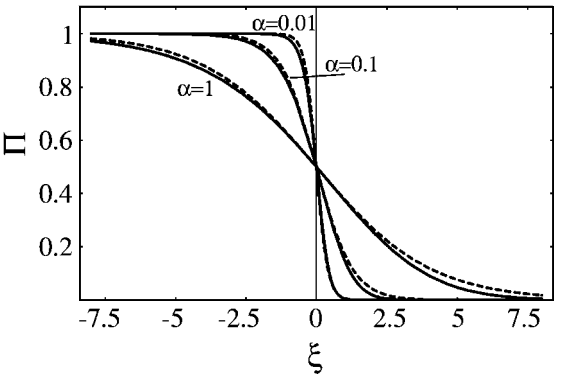


Fig. 1. The form of the phytoplankton front for different values on the diffusion coefficient. The full lines are the approximate solution described in Eq. (6) and the dashed lines are high-resolution numerical solutions.

### 2.3. Defining some numerical schemes for the advection–diffusion equation

In the following section, some numerical schemes for the advection–diffusion operator on a regularly spaced grid will be described. The schemes are delineated by writing the horizontal transport in flux form

$$\frac{\partial}{\partial x}\left(-P + \alpha\frac{\partial P}{\partial x}\right) = -\frac{\partial F}{\partial x}. \tag{7}$$

where $F$ is the flux in the $x$-direction. The change at gridpoint $i$ is described by the difference in the fluxes at the sides of the grid cell divided by the volume of the grid point, thus

$$\frac{\partial F}{\partial x} = \frac{-F_{i-1/2} + F_{i+1/2}}{\Delta x}. \tag{8}$$

The flux at the downstream side is given by

$$F_{i+1/2} = P_{i+1/2} - \alpha\left.\frac{\partial P}{\partial x}\right|_{i+1/2}, \tag{9}$$

and the flux at the upstream side is found from a similar expression starting from point $i-1$, i.e., $F_{i-1/2} = F_{(i-1)+1/2}$. The plankton concentration $P$ is only defined at grid points; thus, it is necessary

to find the plankton concentration—and its gradient—in-between grid points. This can be done in a number of ways where each formulation has their merits and drawbacks.

The concentration $P_{i+1/2}$ can be estimated from the concentration at grid points using a Taylor Series, starting from the upstream gridpoint $i$

$$P\left(x_i+\frac{\Delta x}{2}\right)=P(x_i)+\frac{1}{1!}\frac{\partial P}{\partial x}\frac{\Delta x}{2}+\frac{1}{2!}\frac{\partial^2 P}{\partial x^2}\times\left(\frac{\Delta x}{2}\right)^2+\frac{1}{3!}\frac{\partial^3 P}{\partial x^3}\times\left(\frac{\Delta x}{2}\right)^3+\ldots \quad (10)$$

The more terms that are include in the series, the higher is the accuracy of the scheme. With $P_{i+1/2}=P_i$ it follows from Eqs. (7) and (8) that $P'(x)=(-P_{i-1}+P_i)/\Delta x$, which is the upwind scheme for a first-order derivative. Using this scheme to describe the first-order derivative in Eq. (10) it follows that $P_{i+1/2}=(-P_{i-1}+3P_i)/2$, which is a second-order upstream scheme. This scheme does not perform well in the scenario used in this study and it will not be considered any further. By using $P'(x)=(-P_i+P_{i+1})/\Delta x$ to evaluate the first-order derivative in Eq. (10) it follows that $P_{i+1/2}=(P_i+P_{i+1})/2$, which is the well-known second-order central scheme for derivatives, i.e., $P'(x)=(-P_{i+1}-P_{i-1})/(2\Delta x)$. Using the central scheme for the first-order derivative and a "standard" finite difference scheme for the second-order derivative give

$$P_{i+1/2}=P_i+\left(\frac{-P_{i-1}+P_{i+1}}{2}\right)+\left(\frac{P_{i-1}-2P_i+P_{i+1}}{8}\right),$$

which is a third-order upwind scheme sometimes referred to as the Quadratic Upstream Interpolation for Convective Kinematics (QUICK) scheme (Leonard, 1979; Vested et al., 1996).

An artifact with higher order schemes is that the interpolation may produce non-realistic values on $P_{i+1/2}$; e.g., negative values near a sharp front. The form of Eq. (3) implies that the solution is positive definite; thus, if the scheme produces negative values on $P_{i+1/2}$, these values are clipped to be zero. This scheme will conserve the positive definite properties of the solution, and is referred to as modified QUICK scheme.

In order to describe the diffusion, it is necessary to find $P'_{i+1/2}$; a Taylor expansion gives

$$P'\left(x_i+\frac{\Delta x}{2}\right)=P'(x_i)+\frac{1}{1!}\frac{\partial P^2}{\partial x^2}\frac{\Delta x}{2}+\frac{1}{2!}\times\frac{\partial^3 P}{\partial x^3}\left(\frac{\Delta x}{2}\right)^2+\frac{1}{3!}\frac{\partial^4 P}{\partial x^4}\times\left(\frac{\Delta x}{2}\right)^3+\ldots \quad (11)$$

Using $P'(x)=(P_i-P_{i-1})/\Delta x$, the scheme for the second-order derivative becomes $P''(x)=(P_{i+1}-2P+P_{i-1})/\Delta x^2$, using Eqs. (7) and (8).

The time evolution is described with an Adams-Bashforth scheme. The advection, diffusion and plankton growth all have different requirements on the time step. The time step is calculated according to $\Delta t=0.1$ min $(\Delta x,\ \Delta x^2/\alpha,\ 1)$; the quantities in the parenthesis corresponds to the requirement on the time step for advection, diffusion and plankton growth, respectively.

The initial condition is taken to be $P=0$, whereas the boundary conditions are $P=1$ at $x=0$ and $P=0$ as $x\rightarrow\infty$ (i.e., $P=0$ at the rightmost grid point). The numerical solution of Eq. (3) with the above initial and boundary conditions will be investigated in the following two sections.

### 2.4. Numerical solutions with the second-order central scheme

The numerical scheme in the first experiment is set up with the second-order scheme for the diffusion term and the second-order central scheme for the advection term. The experiment is carried out for the case where: (i) the advection term is ignored; (ii) the diffusion is ignored; and (iii) the full model where both advection and diffusion are accounted for. The numerical solutions at $t=100$ for different horizontal resolutions are shown in Fig. 2a–d. The model behavior is remarkably sensitive to the horizontal resolution of the model, and it is apparent that the front of the phytoplankton bloom can move quickly in

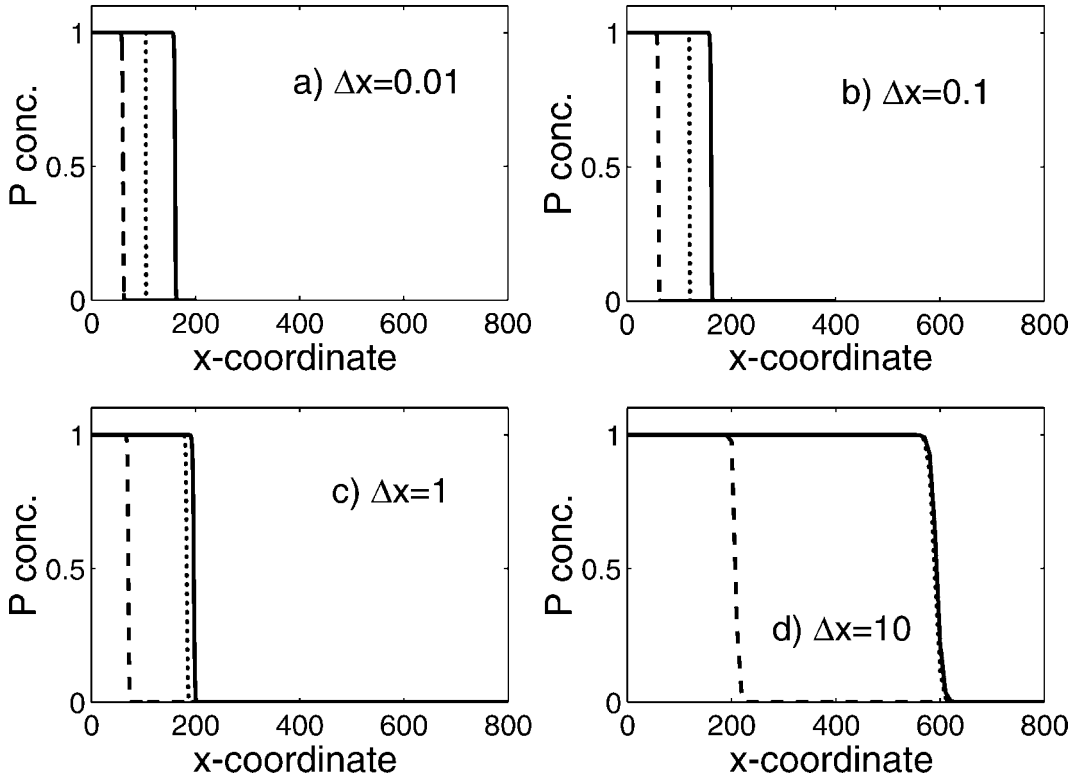


Fig. 2. The phytoplankton concentration at $t=100$ for different sizes of the horizontal grid. Shown are the cases with $\Delta x=0.01$, 0.1, 1, 10, respectively. Each figure displays the solution where: (i) advection is tuned off (dashed line); (ii) diffusion is turned off (dotted line); and (iii) the solution of the full model (full line). From the figure, it is evident that the numerical solution is highly dependent on the horizontal resolution.

the low-resolution case. The conclusion is that the front of the phytoplankton can move much faster than the actual speed of advection in the system if the horizontal resolution is too coarse. Furthermore, by comparing the high- and low-resolution experiments (Fig. 2a–d), it is obvious that the high advection speed represents an unrealistic feature of the numerical solution.

The importance of the advection scheme for the model solution is further investigated in Fig. 3. The advection schemes used in this experiment are the first-order upwind scheme, the second-order central difference scheme, and the third-order QUICK upwind scheme with and without the clipping of negative fluxes (i.e., conservation of the positive definite properties of the solution). It is interesting to note that higher order advection schemes may not improve the accuracy of the numerical solution. The QUICK scheme actually performs worse than the

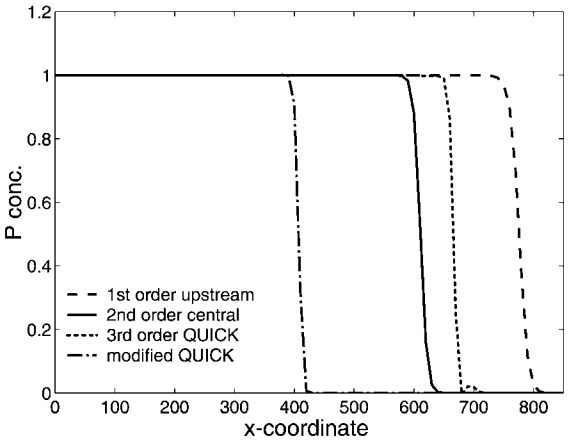


Fig. 3. The advection/growth of phytoplankton for different advection schemes. For these experiments, the resolution is $\Delta x=10$ and an Adams-Bashforth scheme is used for the time derivative.

second-order central scheme at low resolution. It is also evident that the modified QUICK scheme performs better than the other schemes showing that a careful design of the scheme may improve the accuracy of the solution. However, it should be noted that the speed of the front for the modified QUICK scheme is almost a factor 3 too high at low resolution. Thus, there are some indications that there is a fundamental problem with the coarse-resolution finite-difference representation of Eq. (3) and that the use of higher orders schemes may not fully solve the problem.

### 2.5. Speed of the front

The speed of the front as a function of the horizontal resolution is displayed in Fig. 4a–d. For high resolutions (small $\Delta x$), the front moves with a speed of about $1+2\sqrt{\alpha}$ in agreement with theoretical predictions. However, at lower resolution the speed of the front increases, and it is apparent that the numerical experiments cannot describe the relevant processes of the system. The figure shows that the simple upwind scheme performs worst of the tested schemes; this is partly due to the strong numerical diffusivity of this scheme. Overall, the modified QUICK scheme performs best whereas the original QUICK scheme is similar or worse than the second-order central scheme. The increase in the frontal advection speed at low resolution is mainly due to problems with the advection scheme. For instance, the advection speed at low resolution is almost independent of the value of $\alpha$ (see also Fig. 2).

It should be noted that the resolution needed to describe the front depends on $\alpha$. If $\alpha$ is large, the advection of the front is dominated by the diffusion process and a resolution of order $\sqrt{\alpha}$ will suffice to describe the system (Eq. 6). This is seen in Fig. 4d where the advection speed is correctly described up to $\Delta x \sim 3$ for $\alpha = 10$. However, for small $\alpha$, the movement of the front is dominated by advection and there

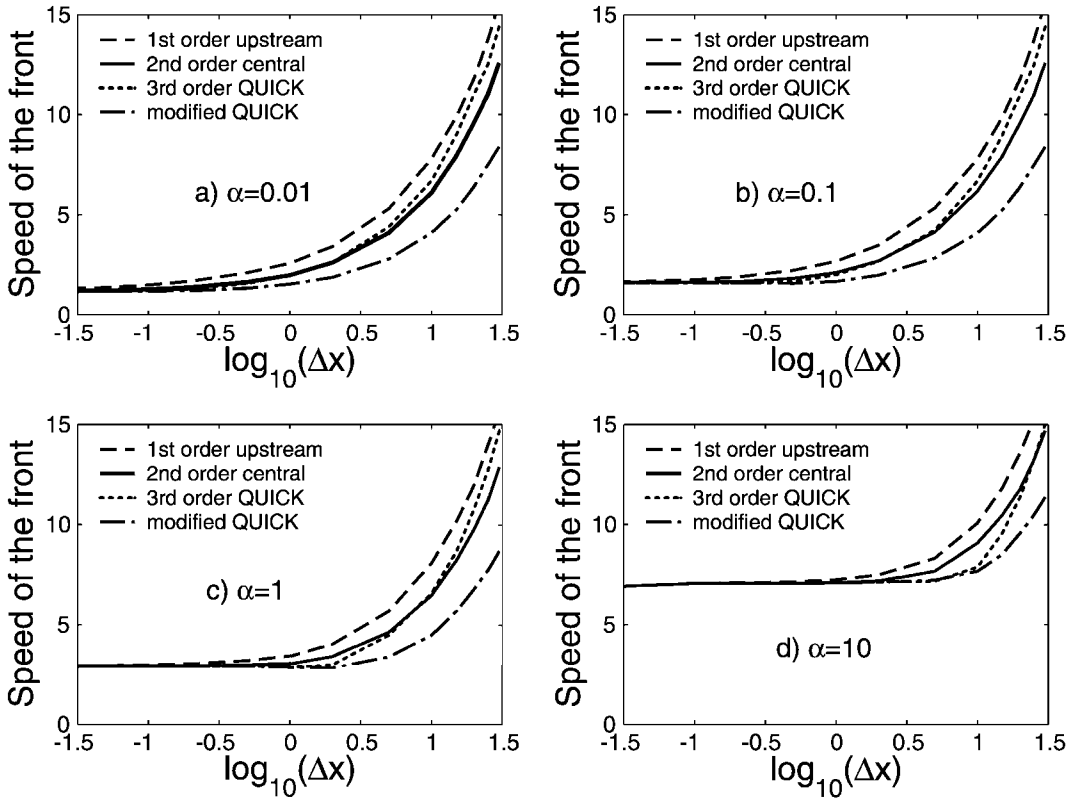


Fig. 4. The speed of the front as a function of the horizontal resolution. The figures represent different values on the diffusion coefficient $\alpha$.

is another condition for the resolution. For instance, with $\alpha = 0.01$ the advection speed of the front is well reproduced up to $\Delta x \sim 1$ for the modified QUICK scheme (Fig. 4a). Experiments with very small values of $\alpha$ show similar results.

Is it possible to find a more rigorous estimate on the $\Delta x$ that would describe the moving plankton front for small values on $\alpha$? Let us assume that the front has value $P = 0.5$ at a certain gridpoint $k$, lets further assume that the upstream concentration is close to 1, and that the concentration downstream is close to 0. With this configuration, it follows that $\partial P/\partial x|_{i=k} \approx (0.5,\ 0.5,\ 0.562)\Delta x^{-1}$ for the upwind, central and QUICK schemes, respectively. The net growth of phytoplankton at grid cell $k$ is given by $P(1-P)|_{i=k} = 0.25$. For small diffusion coefficients, the similarity solution predicts that the front is sharp and that the net growth of phytoplankton is very small. Thus, the requirement on the advection scheme is that $\partial P/\partial x \gg P(1-P)|_{i=k}$, which translates to $\Delta x \ll (2,\ 2,\ 2.248)$ for the upwind, central and QUICK schemes, respectively. These requirements indicate that $\Delta x$ should be, say, 0.2 to reproduce the dynamics of the front in a correct way. However, a more stringent analysis must involve the time development of the front (it turns out that $P_k = 0.5$ represents the worst case scenario). Thus, it is likely that $\Delta x \sim 1$ will reproduce the dynamics of the front in a fairly correct way although $\Delta x \sim 0.1$ is probably required to represent the front with high accuracy. These conclusions agree with the numerical experiments presented in Fig. 4.

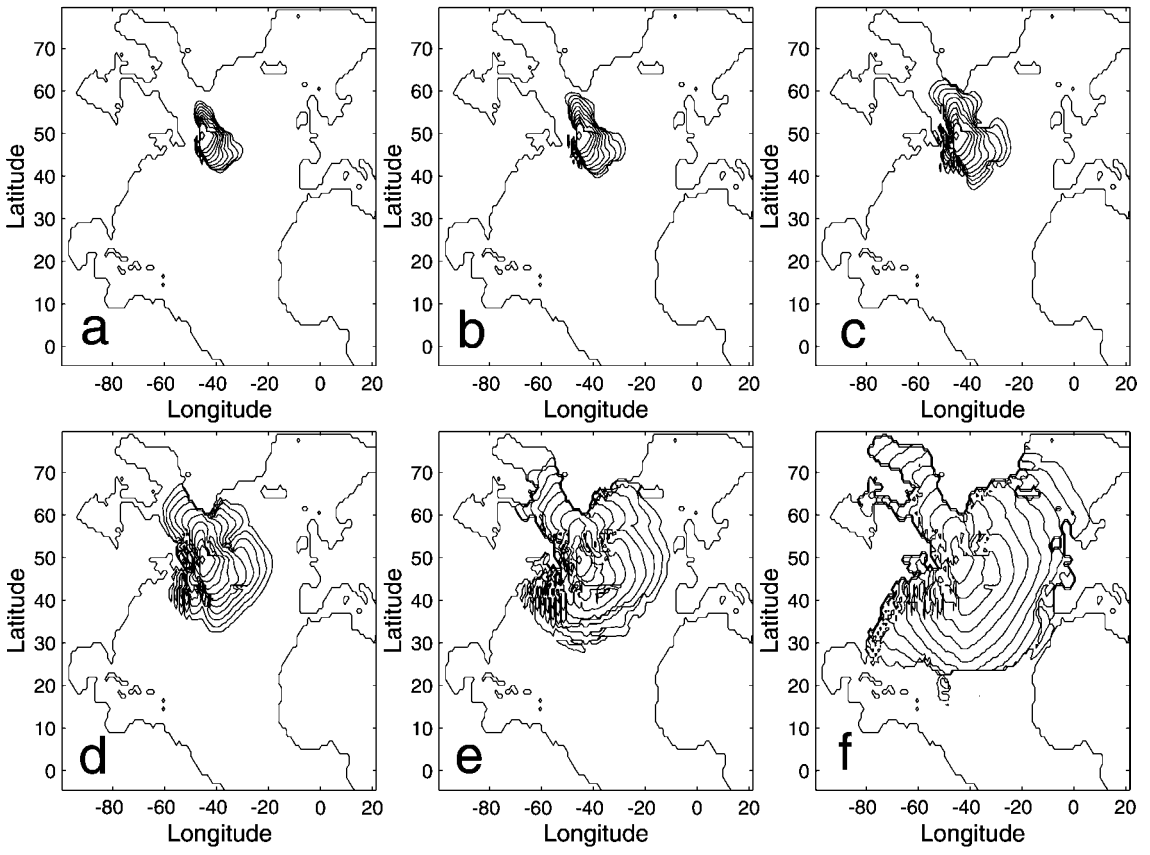


Fig. 5. The dispersion of phytoplankton from a single cell. The figures show the front of the plankton bloom for every 10th day. The figures a–f show experiments with phytoplankton growth and metabolism rates corresponding to $\gamma_P = 1/32,\ 1/16,\ 1/8,\ 1/4,\ 1/2,\ 1\ \text{day}^{-1}$ and $\mu_P = 1/32,\ 1/16,\ 1/8,\ 1/4,\ 1/2,\ 1\ (\mu\text{mol/kg day})^{-1}$, respectively.

## 3. Some results from a general circulation model

The discussion has so far been rather academic, and it is of some interest to study a more realistic situation. Thus, the MIT biogeochemical ocean model with a medium-resolution of $1 \times 1^\circ$ will be used in some semi-realistic model experiments. The model is based on a finite difference representation of the dynamical equations that are relevant for ocean dynamics (Follows et al., 1996; Marshall et al., 1997a,b). The model is used in an off-line mode for the phytoplankton dynamics; the advection is described by the central difference scheme, and the Adams-Bashforth scheme is used for the time evolution.

### 3.1. Dispersion from a single cell

In this experiment, a single grid-point is assigned $P=1$; all other grid points are set to zero. The experiment starts at day 100, and the time evolutions for the first 100 days are shown in Fig. 5a–f. The same experiment is considered for six different growth (and metabolism/grazing) rates, and it is evident that the phytoplankton bloom moves faster if the plankton have high growth rates. Notably, the dispersion rate for the lowest growth rates are consistent with the advection velocities displayed in Fig. 6, whereas the dispersion rate for the high growth rates are significantly faster than the ocean currents. The experiments show that unrealistic solutions may occur in coarse resolution ocean models under the prescribed condition. Repeated experiments where either the advection or the diffusion terms are removed show that the advection and diffusion are about equally responsible for the quick dispersion of the phytoplankton at high growth rates.

### 3.2. On the dynamics of the spring bloom

To describe a realistic evolution of the phytoplankton plankton bloom, dissolved nutrients is included in the model and the phytoplankton growth rate is taken to depend on the light field and the nutrient availability (the rate constant is 1.1 day$^{-1}$ at 10 °C and depends on the temperature; Eppley, 1972). The plankton metabolism contains a linear part (rate constant 0.2 day$^{-1}$) and a quadratic part (rate constant 0.6 [μmol/kg day]$^{-1}$). To describe the loss of nutrients from the upper layer, 60% of the metabolism is remineralized at the same depth as the production

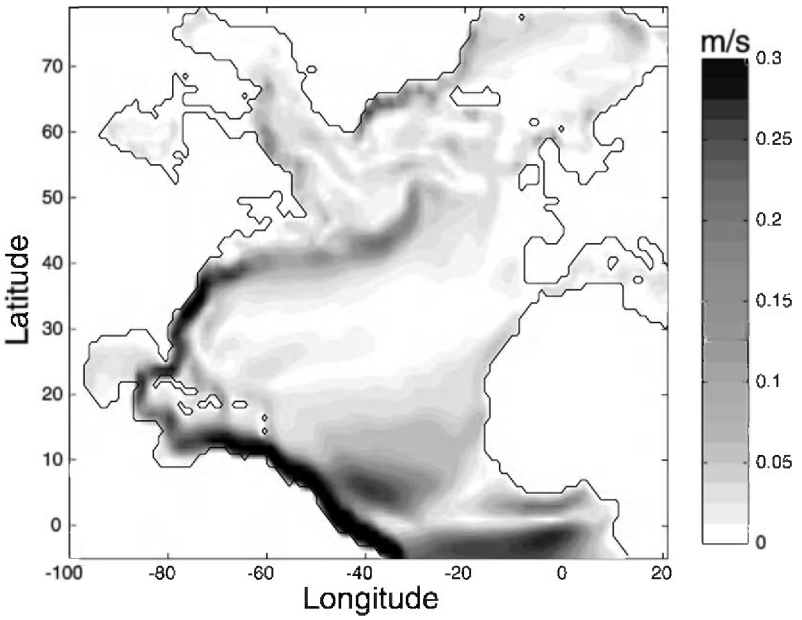


Fig. 6. The magnitude of the velocity field for April.

occurs; the remaining part is remineralized at deeper layers according to a prescribed depth profile.

The model is run with this setup for 20 years and the northward propagation of the plankton bloom is displayed with thin lines in Fig. 7a–f. Compared with a more complicated ecosystem model (Dutkiewicz et al., 2001), it may be noted that the plankton bloom start somewhat later in the northern areas with this simple model. However, the aim of this study is to investigate the numerical properties of coarse resolution ocean models, not to make predictions on the timing of the spring bloom.

According to the experiments in Section 2, it seems plausible that falsely induced numerical advection may be important for the initiation of the spring bloom. The origin of the plankton that makes up the spring bloom in the model is investigated in an experiment with two indistinguishable plankton. The plankton dynamics are formulated such that the sum of the two plankton—named $P_1$ and $P_2$—reveals the dynamic of the model with one plankton species (i.e., $P$ can be substituted with $P_1+P_2$ in Eq. (1)). The changes due to growth and loss for each plankton is taken as proportional to their relative abundance (note that the relative ratios of $P_1$ and $P_2$ are conserved in the biological processes). The experiment with this setup is started on March 1, and the total plankton concentration is taken from the experiment with one plankton species. The initial plankton concentration is divided into plankton $P_1$ and $P_2$ as follows: plankton concentrations that are smaller than 0.01 are set to plankton $P_1$; all other concentrations are assigned to plankton $P_2$. Thus, plankton $P_1$ dominates in the northern areas and is zero elsewhere; plankton $P_2$ dominates in the southern region and is zero in the northern regions (Fig. 7a).

The evolution of plankton $P_1$ and $P_2$ are shown in Fig. 7a–f. Both plankton populations increase their presence during the spring bloom; however, it turns out that plankton $P_2$ (originally the southernmost population) dominates the spring bloom overall. It is evident that a significant part of the spring bloom in the model is initialized by horizontal advection (species $P_2$) rather than emerging from local conditions (species $P_1$). The experiment also shows that the two plankton species are not separated by fronts in the

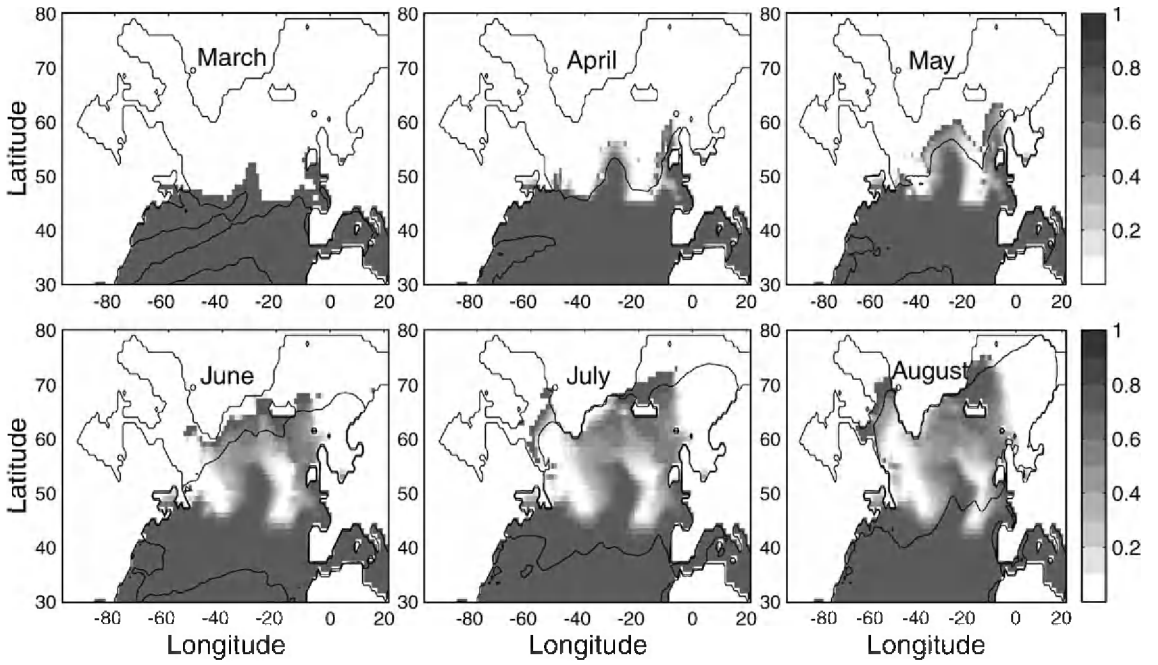


Fig. 7. The evolution of the spring bloom. The thin lines represents the isoline of the $P=0.1$ μmol/kg level. The ratio $P_2/(P_1+P_2)$ is indicated by the gray shade. If this ratio is close to 1, the system is dominated by plankton species $P_2$; if the ratio is close to zero, the system is dominated by plankton species $P_1$.

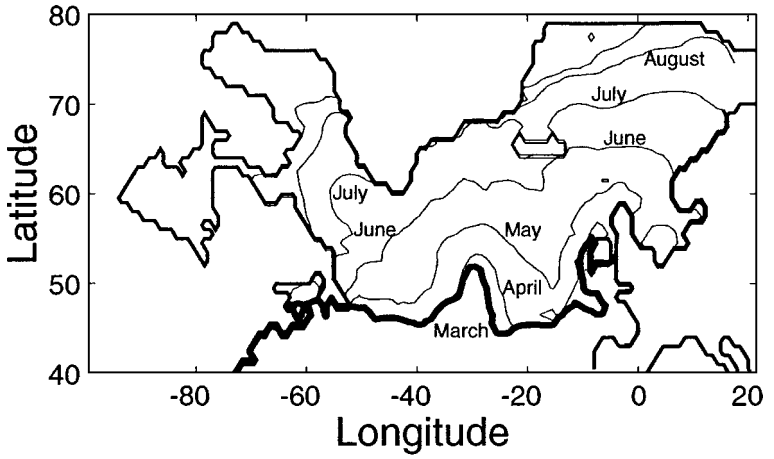


Fig. 8. Invasion of plankton into the North Atlantic. In this experiment, the phytoplankton concentration north of the thick line is set to zero on March 1. The modeled front of the phytoplankton bloom (the $P=0.1$ μmol/kg isoline) for the following months are shown in the figure.

model. The high diffusivity in the ocean model—in combination with high growth rates—probably acts to mix different plankton species in an efficient way.

The initiation of the spring bloom is further investigated in an experiment where the plankton concentration is set to zero in the northern areas (i.e., the region that was occupied by plankton $P_1$ in the previous experiment). The position of the plankton bloom is displayed in Fig. 8, and the experiment reveal that the spring bloom proceeds northwards with a speed that is not unlike the northward propagation in the original experiment. Thus, the numerical deficiencies of the model may well produce results that interfere with a more correct dynamic. (A similar experiment with a passive tracer shows that the ocean currents will only carry the plankton a very short distance, say 10–20% of the distance shown in Fig. 8.) Although the delineated situation is somewhat simplified, the experiments clearly show that the numerical artifacts of low-resolution models may seed plankton to surrounding areas in an unphysical way.

## 4. Discussion

In this study, some unphysical behavior concerning the advection and diffusion of phytoplankton in coarse resolution ocean models is described. The situation arises when there is a combination of high phytoplankton growth rate, zero phytoplankton concentration over a large area, and coarse horizontal resolution. For the prescribed situation, the advection and diffusion will act to transport plankton into low concentration areas. When the advection and diffusion processes are described in a finite difference scheme with coarse resolution, these processes may act to seed a large area with phytoplankton from which a population will grow rapidly. Once the plankton population in a grid cell reaches a high concentration, the signal can move on to the next box. The result is that the front of the plankton bloom can move at a speed that is much higher than the speed of the ocean currents.

A situation where the fast-moving plankton bloom may interfere with a more truthful description of the system is the case when the dynamics of a specific plankton species should be described. An example is the advection of large neritic diatoms. One of the characteristics of neritic diatoms is that they change state in the late part of the bloom (e.g., when they reach low nutrient concentrations) and sink quickly towards to bottom of the ocean (Alldredge et al., 1995; Alldredge and Gotschalk, 1989). It is reasonable to assume that this is a part of their survival strategy (Sambrotto et al., 1986)—a strategy that is probably an adaptation to shallow shelf areas but will work poorly in the open ocean. If the origins of these plankton species are at some shelf area, it is important to study how they are transported to the central parts

of the ocean. The experiments with the GCM model suggest that the incorporation of fast growing shelf-adapted diatoms in a coarse resolution model may produce some questionable results on their dispersion rate (Fig. 5). Thus, it may be difficult to describe the dynamics of these large diatoms in a coarse-resolution model. This is unfortunate as (neritic) diatoms potentially are very important for the flux of organic carbon to the deep ocean (e.g., Michaels and Silver, 1988).

Another situation where numerical artifacts may interfere with results that are more realistic is during the spring bloom. In the North Atlantic, the spring bloom travels northward faster than the ocean currents. The direct implication is that local conditions will dominate in the initial part of the plankton bloom. Most likely, the phytoplankton population at the end of the winter season is the result of a complex interplay between survival adaptation of phytoplankton, advection by ocean currents, and the mixing dynamics of the uppermost ocean (Townsend et al., 1994). However, in coarse-resolution models, the horizontal advection–diffusion may support a seed population to these areas in an unphysical way, which makes it impossible to study these intricate wintertime dynamics. Accordingly, the importance of winter processes on the phytoplankton spring bloom can probably not be studied with a coarse resolution ocean model.

In order to model the moving plankton front in a correct way the dominant processes of the system must be properly described. If diffusion is the dominant process for the plankton transport, it can be shown that resolution should at least be of order $\sqrt{D/\gamma_P}$ to resolve the front. If advection is the dominant transport mechanism for plankton, the resolution of the model should be at least on the order of $U/\gamma_P$, although some scheme may require higher resolution (Fig. 4). It should be noted that the largest of $\sqrt{D/\gamma_P}$ or $U/\gamma_P$ will suffice to describe the dominant process of the system (Fig. 4). Assuming that the advection velocity in the ocean is about 0.1 m/s and that the growth rate for phytoplankton is on the order of 1 $day^{-1}$, it follows that the horizontal resolution of the model should be at least 8 km (preferably less) to capture the advection/growth of phytoplankton in a purposeful way. Given that the resolution of most general circulation models are significantly less than 8 km, it follows that the biological component in these coarse resolution ocean models requires a careful design and interpretation to circumvent false results.

## Acknowledgements

I would like to thank Dr. Mick Follows for stimulating discussions and helpful comments on an early version of the manuscript. I am also thankful to the Knut and Alice Wallenberg foundation that provided a postdoctoral fellowship to MIT. Two anonymous reviewers also made important contributions for the outcome of this paper.

## References

Alldredge, A.L., Gotschalk, C.C., 1989. Direct observations of the mass flocculation of diatom blooms: characteristics, settling velocities and formation of diatom aggregates. Deep-Sea Res. 36, 159–171.

Alldredge, A.L., Gotschalk, C., Passow, U., Riebesell, U., 1995. Mass aggregation of diatom blooms: insights from a mesocosm study. Deep-Sea Res., Part II 42, 9–27.

Broström, G., 2000. The role of the seasonal cycles for the air–sea exchange of $CO_2$. Mar. Chem. 72, 151–169.

Broström, G., Drange, H., 2000. On the mathematical formulation of the oceanic plankton system. Sarsia 85, 211–225.

Doney, S.C., Glover, D.M., Najjar, R.G., 1996. A new coupled, one-dimensional biological–physical model for the upper ocean: applications to the JGOFS Bermuda Atlantic Time-series Study (BATS) site. Deep-Sea Res., Part II 43, 591–624.

Dutkiewicz, S., Follows, M., Marshall, J., Gregg, W.W., 2001. Interannual variability of phytoplankton abundances in the North Atlantic. Deep-Sea Res., Part II 48, 2323–2344.

Eppley, R.W., 1972. Temperature and phytoplankton growth in the sea. Fish. Bull. 70, 1063–1085.

Evans, G., Parslow, T., 1985. A model of annual plankton cycles. Biol. Oceanogr. 3, 327–347.

Fasham, M.J.R., 1995. Variations in the seasonal cycle of biological production in subarctic oceans: a model sensitivity analysis. Deep-Sea Res. 42, 1111–1149.

Fasham, M.J.R., Ducklow, H.W., McKelvie, S.M., 1990. A nitrogen-based model of plankton dynamics in the oceanic mixed layer. J. Mar. Res. 48, 591–639.

Fasham, M.J.R., Sarmiento, J.L., Slater, R.D., Ducklow, H.W., Williams, R., 1993. Ecosystem behavior at Bermuda Station 'S' and Ocean Weather Station 'India': a general circulation model and observational analysis. Global Biogeochem. Cycles 7, 379–415.

Follows, M.J., Williams, R.G., Marshall, J.C., 1996. The solubility pump of carbon in the subtropical gyre of the North Atlantic. J. Mar. Res. 54, 605–630.

Leonard, B.P., 1979. A stable and accurate convective modelling procedure based on quadratic upstream interpolation. Comput. Methods Appl. Mech. Eng. 19, 59–98.

Marshall, J., Adcroft, A., Hill, C., Perelman, L., Heisey, C., 1997a. A finite-volume, incompressible Navier Stokes model for studies of the ocean on parallel computers. J. Geophys. Res. 102, 5753–5766.

Marshall, J., Hill, C., Perelman, L., Adcroft, A., 1997b. Hydrostatic, quasi-hydrostatic, and nonhydrostatic ocean modeling. J. Geophys. Res. 102, 5733–5752.

McGillicuddy Jr., D.J., Robinson, A.R., 1998. Interaction between the oceanic mesoscale and the surface mixed layer. Dyn. Atmos. Ocean. 27, 549–574.

McGillicuddy, D.J.J., Robinson, A.R., McCarthy, J.J., 1995. Coupled physical and biological modelling of the spring bloom in the North Atlantic (II): three dimensional bloom and post-bloom processes. Deep-Sea Res. 42, 1359–1398.

McGillicuddy Jr., D.J., Robinson, A.R., Siegel, D.A., Jannasch, H.W., Johnson, R., Dickey, T.D., McNeil, J., Michaels, A.F., Knap, A.H., 1998. Influence of mesoscale eddies on new production in the Sargasso Sea. Nature 394, 263–266.

Michaels, A.F., Silver, M.W., 1988. Primary production, sinking fluxes and the microbial food web. Deep-Sea Res. 35, 473– 490.

Murray, J.D., 1989. Mathematical Biology. Springer Verlag, New York, 767 pp.

Oberhuber, J.M., 1993. Simulation of the Atlantic circulation with a coupled sea ice-mixed layer-isopycnal general circulation model: II. Model experiment. J. Phys. Oceanogr. 23, 830–845.

Oschlies, A., Garcon, V., 1998. Eddy-influenced enhancement of primary production in a model of the North Atlantic Ocean. Nature 394, 266–269.

Sambrotto, R.N., Niebauer, H.J., Goering, J.J., Iverson, R.L., 1986. The relationship among vertical mixing, nitrate uptake, and growth during the spring phytoplankton bloom in the southeast Bering Sea middle shelf. Cont. Shelf Res. 5, 161–198.

Sambrotto, R.N., Martin, J.H., Broenkow, W.W., Carlson, C., Fitzwater, S.E., 1993. Nitrate utilization in surface waters of the Iceland Basin during spring and summer of 1989. Deep-Sea Res., Part II 40, 441–457.

Stammer, D., Wunsch, C., Giering, R., Zhang, Q., Marotzke, J., Marshall, J., Hill, C., 1997. The global ocean circulation estimated from TOPEX/POSEIDON altimetry and a general circulation model. 49, Center for Global Change, MIT.

Townsend, D.W., Cammen, L.M., Holligan, P.M., Campbell, D.E., Pettigrew, N.R., 1994. Causes and consequences of variability in the timing of spring phytoplankton blooms. Deep-Sea Res. 41, 747–765.

Vested, H.J., Baretta, J.W., Ekebjærg, L.C., Labrosse, A., 1996. Coupling of hydrodynamical transport and ecological models for 2D horizontal flow. J. Mar. Syst. 8, 255–267.